Chaotic Resonance in Izhikevich Neural Network Motifs Under Electromagnetic Induction

Guowei Wang
Central China Normal University
Lijian Yang
Central China Normal University
Xuan Zhan
Central China Normal University
Anbang Li
Central China Normal University
Ya Jia (jiay@mail.ccnu.edu.cn)
Central China Normal University School of Physics https://orcid.org/0000-0002-2818-9074

Research Article

Keywords: Izhikevich neuron model, Chaotic resonance, Electromagnetic induction, 27 Fourier coefficient, Lorenz system, Network motifs

Posted Date: September 17th, 2021

DOI: https://doi.org/10.21203/rs.3.rs-895256/v1

Version of Record: A version of this preprint was published at Nonlinear Dynamics on January 29th, 2022. See the published version at https://doi.org/10.1007/s11071-021-07150-3.

Chaotic resonance in Izhikevich neural network motifs under electromagnetic induction

Guowei Wang, Lijian Yang, Xuan Zhan, Anbang Li, Ya Jia*

Department of Physics, Central China Normal University, Wuhan 430079, China

Abstract: Chaotic resonance (CR) is the response of a nonlinear system to weak signals enhanced by internal or external chaotic activity (such as the signal derived from Lorenz system). In this paper, the triple-neuron feed-forward loop (FFL) Izhikevich neural network motifs with eight types are constructed as the nonlinear systems, and the effects of EMI on CR phenomenon in FFL neuronal network motifs are studied. It is found that both the single Izhikevich neural model under electromagnetic induction (EMI) and its network motifs exhibit CR phenomenon depending on the chaotic current intensity. There exists an optimal chaotic current intensity ensuring the best detection of weak signal in single Izhikevich neuron or its network motifs via CR. The EMI can enhance the ability of neuron to detect weak signals. For T1-FFL and T2-FFL motifs, the adjustment of EMI parameters makes T2-FFL show a more obvious CR phenomenon than that for T1-FFL motifs, which is different from the impact of system parameters (e.g., the weak signal frequency, the coupling strength, and the time delay) on CR. Another interesting phenomenon is that the variation of CR with time delay exhibits quasi periodic characteristics. Our results showed that CR effect is a robust phenomenon which is observed in both single Izhikevich neuron and network motifs, which might help one understand how to improve the ability of weak signal detection and propagation in neuronal system.

Keywords: Izhikevich neuron model; Chaotic resonance; Electromagnetic induction; Fourier coefficient; Lorenz system; Network motifs

* Corresponding author: jiay@mail.ccnu.edu.cn

1. Introduction

Resonance is a term which is used with very high frequency in physics [1]. It refers to the situation that a system vibrates with a greater amplitude than other frequencies and wavelengths at a specific frequency and wavelength [2]. At the resonance frequency and resonance wavelength, a small periodic vibration can produce a large vibration [3]. In general, a system (whether mechanical, thermal or electronic) has multiple resonance frequencies, and it is easy to vibrate at these frequencies and difficult to vibrate at other frequencies [4]. The concept of "stochastic resonance" (SR) was first proposed by Benzi *et al* [5] and used to explain the Quaternary glacier problem. After that, it was widely used to describe the phenomenon that the presence of internal noise or external noise in nonlinear system can increase the response of the system output [6]. In the process of signal analysis, noise is often regarded as a nuisance, because the presence of noise reduces the signal-to-noise ratio and affects the extraction of useful information [7, 8]. However, in some specific nonlinear systems, the presence of noise can enhance the detection ability of weak signals [9, 10].

It is well known that the occurrence of resonance must meet three conditions at the same time, namely the existence of nonlinear system, noise and weak signal [11]. With the deepening of research, it is found that the role of noise can be replaced by high-frequency (HF) signal, so that in this case the resonance phenomenon of nonlinear system can also be observed [12, 13]. This resonance phenomenon is called vibrational resonance (VR), from which one can observe the system's response to a weak low-frequency (LF) signal become maximal by an appropriate choice of vibration amplitude for the HF signal [14, 15]. As far as we know, vibration resonance refers to the mechanism that one can make use of the optimal amplitude of HF driving to enhance the response of excitable system to LF sub-threshold signals, therefore the utilization of double-frequency signal to explore signal detection and transmission has been widely studied [16, 17]. This double-frequency signal exists in many different fields, including brain dynamics, telecommunications, neural networks and so on [18, 19].

The brain's cognitive functions (such as working memory, selective attention and sensory coding) are realized through irregular neuronal discharges [20]. For neuroscience, exploring, revealing and understanding brain connections is one of the most important problems [21]. Different interconnected states are considered to be the

basis of different cognitive functions of the human brain [22]. Meanwhile, some neurological diseases, such as Parkinson's disease, have been proved to be related to brain connectivity disorders [23]. For nervous system or neural network, it contains a large number of neurons in different discharge states, and these neurons receive and produce different neural signals in the process of interaction with each other [24]. In this way, the signal transmission of the nervous system becomes complex and chaotic, resulting in some neurons in chaotic discharge state [25]. For nervous system, chaotic signal comes from two parts, one of which is the chaotic signal generated by external chaotic activities, and the other is the chaotic signal generated by internal chaotic activities [26]. Recent studies have shown that the response to weak signals can be amplified by chaotic activity rather than noise or HF driving, and this phenomenon is defined as chaotic resonance (CR) [27, 28].

On the one hand, it was found that CR effect is a robust phenomenon, which can be observed in both single neuron and neural networks [29]. In 2019, Baysal *et al*. [30] studied the influence of external chaotic signals on weak signal detection performance of Hodgkin-Huxley (HH) neurons through numerical simulation. After that, they investigated the effects of autapse on CR phenomenon in single HH neuron and small-world (SW) neuronal networks in 2020 [31]. Tokuda *et al*. [32] investigated the role of CR in cerebellar learning, they pointed out that CR widens the range of noise intensity within which efficient learning can be realized, and they suggested that the spiking activity induced by chaos can be more economical than that induced by noise from an energetic viewpoint. CR was found by Nobukawa and Nishimura [33] to arise with appropriate coupling strength for weak signal and have the frequency response characteristic as with general resonance phenomena. Chew *et al*. [29] considered the resonant effects of chaotic fluctuations on a strongly damped particle in a bistable potential driven by weak sinusoidal perturbation. Kazuyoshi *et al*. [34] studied CR in forced Chua's oscillators. A large number of studies further show the universality and importance of CR [7].

On the other hand, as the basic structural unit of neural network, neuron performs its function in a network receiving contacts from about 10^4 presynaptic neurons [35]. Such a dense connectivity profile for a single neuron may lead to a huge and complex neuronal topology, which may be difficult to understand the potential mechanism of neural function and disease [36]. A large number of experimental data from neuroanatomical research have found that neural networks include some

recurrent microcircuit topologies, known as network motifs, which are used as feature building modules of complex networks [37, 38]. Jiao *et al*. [39] pointed out that network motifs play an important role in network classification and network attribute analysis, and they proposed a method for analyzing the effective connectivity of functional magnetic resonance imaging data by using network motifs. Milo *et al.* [40] investigated motifs in networks from biochemistry, neurobiology, ecology and engineering. Alon *et al.* [41] reviewed network motifs and their functions, and focused on using experiments to study neural motifs. Therefore, it is generally believed that a clear explanation of the dynamic and functional characteristics of these network motifs can be used as the first step to understand large networks [42, 43].

Although there are studies on CR in single neuron or SW neural network, there are few studies on CR in neural network motifs [44, 45]. In particular, there is basically no research on CR of Izhikevich neural network motifs under the action of EMI [46]. It is very important to investigate CR phenomenon of network motifs and the influence of EMI on CR, and it has guiding significance for the detection performance and transmission ability of neural signals in chaotic environment [47]. Thus, some interesting questions now arise: Is there CR in the Izhikevich neuronal systems? How does the chaotic signal affect the membrane potential of Izhikevich neuronal model under EMI? What are the effects of both chaotic signal and EMI on the triple-neuron feed-forward loop (FFL) neural network motifs?

In this paper, to address above issues, the triple-neuron FFL Izhikevich neural network motifs are constructed, and the effects of EMI on CR in single Izhikevich neural model and Izhikevich network motifs with eight types are investigated, respectively. Our results might provide some theoretical support for construction of large-scale neural networks and detection or transmission of neural information.

2. Model description

2.1 Izhikevich neural model in the presence of chaotic current

Izhikevich neural model is a neuronal discharge model proposed by Eugune M. Izhikevich [48] in 2004, which combines the advantages of Integrate-and Fire (IF) neuronal model [49] and HH neuronal model [50]. It is not only close to the discharge

characteristics of real biological neurons, but also convenient for large-scale simulation [51]. In 2007, Izhikevich and Gerald M. Edelman successfully simulated the thalamocortical system of mammals by using Izhikevich neural model [52]. Considering that the firing neurons of this model have the characteristics of associative memory, and it is closer to real biological neurons, so it has become the focus of scientific research [53].

When considering the existence of chaotic signal and weak signal, Izhikevich neuronal model is a two-dimensional system of ordinary differential equations, which is governed by the following two equations [54]:

$$\begin{aligned} \frac{dv}{dt} &= 0.04v^2 + 5v + 140 - u + I_{syn} + I_{ext}, \\ \frac{du}{dt} &= a(bv - u). \end{aligned} \tag{1}$$

with the auxiliary after-spike resetting

$$\text{if } v \geq 30mV \text{ , then } \begin{cases} v = c, \\ u = u + d. \end{cases} \tag{2}$$

where v and u are dimensionless variables, and v represents the membrane potential of neuron, u denotes the membrane recovery variable. Once if the peak of membrane potential reaches its peak ($+30mV$), the membrane potential and recovery variable are reset according to Eq. (2) [55].

Here, a, b, c, d are four dimensionless parameters which are used to determine the neuron type [56]. On the basis of previous original literature, parameter a is used to describe the time scale of recovery variable u, the parameter b describes the sensitivity of recovery variable u to subthreshold fluctuations of membrane potential v [57].

Regular spiking (RS) neurons (a = 0.02, b = 0.2, c = −65, d = 8) are the most typical neurons in cortex, and they are used to model the excitatory neurons [58]. Fast spiking (FS) neurons (a = 0.1, b = 0.2, c = −65, d = 2) can fire periodic trains of action potentials with extremely high frequency practically without any adaptation (slowing down), and they are utilized to model inhibitory neurons [59].

I_{ext} is the weak signal that applied to Izhikevich neuron, with the form of $I_{ext} = A\sin(\omega t)$ [60]. In which A is the amplitude of weak signal and ω is frequency of weak signal [61]. Neurons interact with the external environment, so they may receive some nerve signals from the surrounding environment, and the total synaptic input received

from the environmental neurons can be introduced into system by $I_{syn} = I_0 + I_{chaos}$ [62]. The total synaptic current I_{syn} consists of two parts, one of which is a constant direct current (DC) stimulation signal, or called slow current; the other part is chaotic current stimulation signal, which can also be called fast current [63].

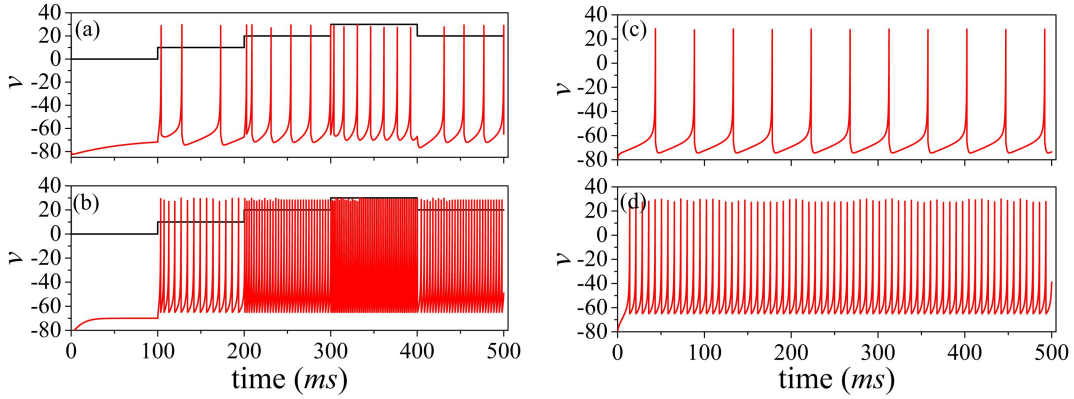

Fig. 1 Evolution of membrane potential versus time of Izhikevich neuron to external current I_0 : (a, c) regular spiking (RS) neuron and (b, d) fast spiking (FS) neuron.

As can be seen from Fig. 1, the size of I_0 controls the frequency of neuronal spike discharge [64]. Therefore, in order to avoid the influence of constant DC signal on chaotic resonance, we define $I_0 = 0$ if there is no special description [27]. Chaotic information generated by environmental neurons is represented by chaotic current I_{chaos}, and its specific form is given by

$$I_{chaos} = \varepsilon x \tag{3}$$

where ε represent chaotic current intensity, and x describes the external chaotic signal derived from Lorenz system [65]. Lorenz system is the first dissipative system with chaotic motion found in numerical experiments, and it is given by following equations [66]:

$$\begin{aligned} \frac{dx}{dt} &= \sigma(y - x), \\ \frac{dy}{dt} &= \rho x - y - xz, \\ \frac{dz}{dt} &= xy - \beta z. \end{aligned} \tag{4}$$

All chaotic signals discussed here are generated by above equations, and the chaotic system parameters are chosen as $\sigma = 10, \rho = 28, \beta = 8/3$.

2.2 Izhikevich neuron model under the effects of EMI

There are a large number of flowing charged ions inside and outside the cell membrane [61, 67]. Therefore, electromagnetic induction (EMI) effect can be introduced into Izhikevich neuronal model according to Faraday's law of electromagnetic induction [68]. Thus, the dynamical equations for the improved Izhikevich neural model are described by as follows [69]:

$$\begin{aligned} \frac{dv}{dt} &= 0.04v^2 + 5v + 140 - u - k_1(\alpha + 3\beta\varphi^2)v + I_{syn} + I_{ext}, \\ \frac{du}{dt} &= a(bv - u), \\ \frac{d\varphi}{dt} &= k_2 v - k_3\varphi. \end{aligned} \tag{5}$$

in which the newly introduced variable φ describes the magnetic flux across membrane, and the term $\rho(\varphi) = \alpha + 3\beta\varphi^2$ is memory conductance of a magnetic flux-controlled memristor [70]. α and β are fixed parameters. k_1 and k_2 are parameters that describe the interaction between membrane potential and magnetic flux [71]. The term $k_3\varphi$ describes the leakage of magnet flux [72]. The total synaptic current I_{syn} and external current I_{ext} are the same as that in Eq. (1) [73].

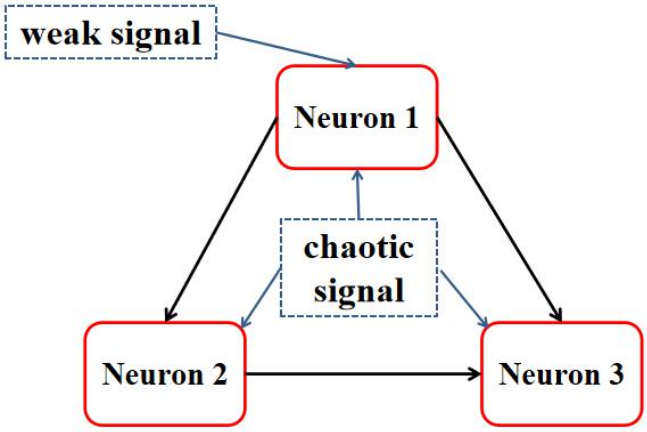

Fig. 2 Connection patterns of the FFL neuronal network motifs: Neuron 1 drives neuron 2, and both jointly drive neuron 3.

2.3 Triple-neuron feed-forward loop (FFL) network motifs

The Izhikevich neural model discussed here is used to build the triple-neuron FFL neuronal network motifs, and the connection patterns is given in Fig. 2 [74]. The interaction between them is that neuron 1 drives neuron 2, and then both jointly drive neuron 3 [75].

The dynamics of the studied motifs is governed by following equations [76]:

$$\begin{aligned}
\frac{dv_i}{dt} &= 0.04v_i^2 + 5v_i + 140 - u_i - k_1(\alpha + 3\beta\varphi_i^2)v_i + I_i^{syn} + I_i^{ext}, \\
\frac{du_i}{dt} &= a_i(b_i v_i - u_i), \\
\frac{d\varphi_i}{dt} &= k_2 v_i - k_3\varphi_i.
\end{aligned} \tag{6}$$

where i = 1, 2, 3 index the neurons. v_i is the membrane potential of the neuron i, u_i represents the membrane recovery of neuron i, φ_i denotes the magnetic flux across membrane of neuron i [77]. The weak signal is input from neuron 1 (which is considered as the input port of the network motifs), the chaotic current are applied to all three neurons, and the output signal is detected on neuron 3 (which is considered as the output port of the network motifs) [78].

I_i^{syn} denotes the total synaptic current and it is the linear sum of all incoming chemical synaptic current onto neuron i from neuron j, which has the form [21]:

$$I_i^{syn} = \sum I_{ij}^{syn} \tag{7}$$

and I_i^{syn} is given as follows:

$$I_i^{syn}(t) = g_{ij} r_j [E_s - v_i(t)] \tag{8}$$

where g_{ij} describes the coupling strength of the synapse from neuron j to neuron i [79]. For simplicity, it is assumed that all connections have the same coupling strength [47]. E_s is defined as the reversal potential, which can be used to determine the type of synapse [80]. The synapse between neurons is expressed in two different forms, i.e., $E_s = 0mV$ for excitatory synapse and $E_s = -80mV$ for inhibitory synapse [81]. What needs to be explained here is how to define the type of synapse. As far as we know, excitatory or inhibitory synapses are determined by the types of pre-synapse neuron according to Ref. [74]. For excitatory neuron, its role is to transmit excitatory neurotransmitters to postsynaptic neurons and cause postsynaptic neurons to respond or discharge or rest duly [82]. On the other hand, for inhibitory neuron, its role is to transmit inhibitory neurotransmitters to postsynaptic neurons and cause postsynaptic neurons to respond accordingly [83].

In Eq. (8), r_j represents the synapse variable, which is the fraction of post-synaptically bound neurotransmitter obeying the first-order kinetics, and it has the form as follows [74]:

$$\frac{dr_j}{dt}=\frac{1-r_j}{1+e^{-(v_j-\tau)}}-\frac{r_j}{10}. \tag{9}$$

where τ represents the length of time delay.

To quantitatively determine the correlation between the weak LF periodic signal and the output activity of Izhikevich neuron and its neural network motifs in the presence of chaotic signal, the Fourier coefficient Q during M = 500 periods of weak signal is calculated as follows [84, 85]:

$$\begin{aligned} Q_{\sin} &= \frac{\omega}{2\pi M}\int_{T_0}^{T_0+\frac{2\pi M}{\omega}} 2v(t)\sin(\omega t)dt, \\ Q_{\cos} &= \frac{\omega}{2\pi M}\int_{T_0}^{T_0+\frac{2\pi M}{\omega}} 2v(t)\cos(\omega t)dt, \\ Q &= \sqrt{Q_{\sin}^2+Q_{\cos}^2}. \end{aligned} \tag{10}$$

where ω is the frequency of weak LF signal, T_0 = 10 is defined as the initial integration time [86]. The maximum of Fourier coefficient Q shows the best phase synchronization between weak input signal and output-neuron firing, which indicates the higher correlation between the weak periodic signal and the output activity of Izhikevich neuron system [87].

According to the existing research conclusions, the value of Q detected at the output neuron 3 is too small and has no research significance if input neuron 1 is an inhibitory neuron [74]. Therefore, only T1-FFL and T2-FFL motifs are discussed in detail in this paper.

3. Results and discussions

In order to fully understand whether there is CR phenomenon in Izhikevich neuronal model and explore the influence of EMI on CR in Izhikevich neural network motifs, the Euler algorithm is used to calculate the Fourier coefficient Q, and the time step is chosen as 0.01 [20]. Unless otherwise specified, other parameters are set as follows, α = 0.4, β = 0.02, k_1 = 0.01, k_2 = 0.01, k_3 = 0.2, τ = 10, A = 0.2, ω = 0.05 [88].

Type of motifs	Neuron 1	Neuron 2	Neuron 3
T1-FFL	E	E	E
T2-FFL	E	I	E
T3-FFL	E	E	I
T4-FFL	E	I	I

T5-FFL	I	E	E
T6-FFL	I	I	E
T7-FFL	I	E	I
T8-FFL	I	I	I

Table 1. Eight possible and frequently discussed FFL motifs types.

By calculating the Fourier coefficient Q, the influence of external chaotic activity obtained by Lorentz system on the weak signal detection performance of single Izhikevich neuron are systematically analyzed [89]. Since the improved model discussed here is closer to the real situation, there are two cases worth studying: one is to consider the role of EMI, and the other is without considering the effects of EMI [90].

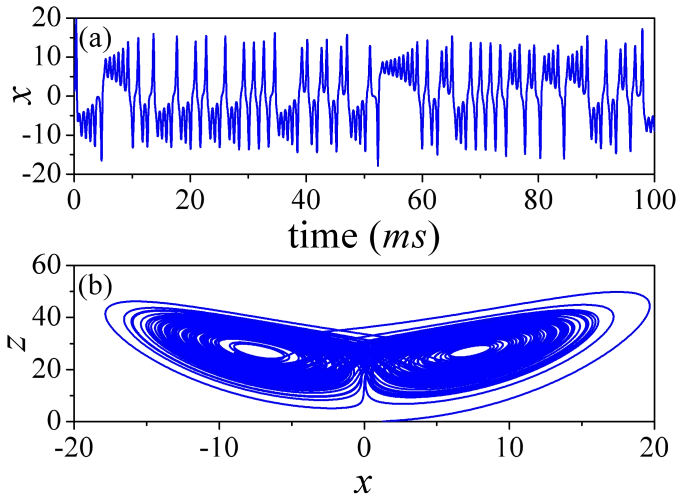

Fig. 3 (a) Time series of Lorenz system; (b) Phase diagram of chaotic Lorenz system.

In order to ensure that the signal input to system meets the research requirements, the parameters of Lorentz system are adjusted to make it in a chaotic oscillation state. In this way, the single Izhikevich neuron model and its neural network motifs are exposed to chaotic signal and weak periodic signal. As shown in Fig. 3, the time series of chaotic signal x derived from Lorenz system and $x-z$ phase plane diagram of chaotic Lorenz system are presented. As can be seen from Fig. 3 that the signal x generated by Lorentz system is indeed in a chaotic oscillation state.

3.1 Chaotic resonance in single Izhikevich neuron

As it is shown in Fig.4, the response of single Izhikevich neuron to weak signal, which is measured by Fourier coefficient Q, is plotted as a function of ε for different frequencies of weak signal. In order to compare the influence of EMI on Fourier

coefficient Q, Fig. 4(a) shows the results considering EMI, while Fig. 4(b) shows the results without considering EMI. As can be seen from Fig. 4, a maximum similar to resonance peak appears when Q changes with the chaotic current intensity ε, which indicates the generation of CR. For both cases, there is an optimal chaotic current intensity to maximize the Q value whether the EMI is considered or not, it means the best detection of weak signal.

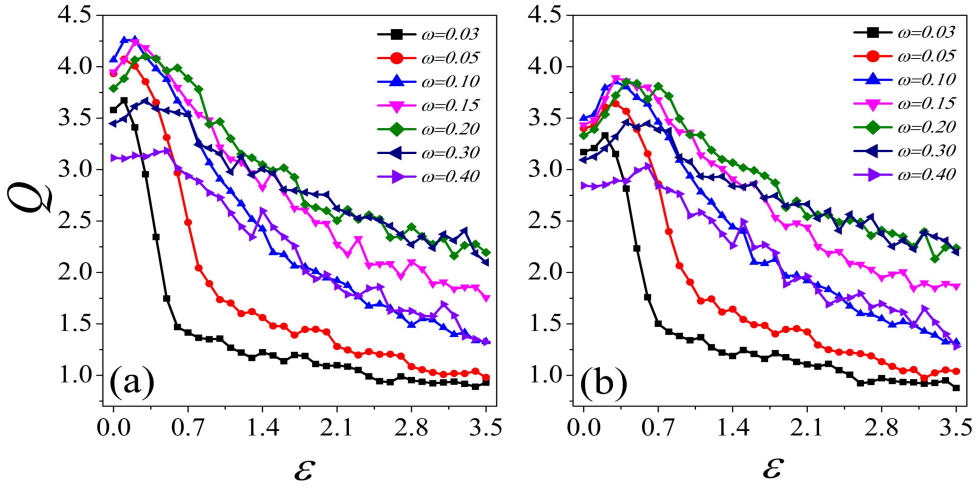

Fig. 4 Response of single Izhikevich neuron to weak signal (Fourier coefficient Q) are plotted as a function of ε for different frequencies of weak signal at A = 1.0. (a) With the effects of EMI and k_1 = 0.01, k_2 = 0.02, k_3 = 0.2; (b) Without the effects of EMI.

Further analysis shows that the Q value is larger in the case of EMI is considered than that in the case of EMI is not considered if the same system parameters are selected. The Q curves exhibit a more sensitive dependence on weak signal frequency ω when EMI is taken into account, as shown in Fig. 4(a). Moreover, the CR phenomenon tends to disappear when the frequency of weak signal is large, and the maximum of Q can hardly be distinguished, which may indicate a phase transition in the neural system. Meanwhile, the larger the value of ω, the larger the ε value corresponding to the maximum value of Q. The most intuitive phenomenon one can see is that the position of the peak gradually moves to right. However, the difference is that the change of Q curve with ε always presents a more perfect bell-shaped-like relationship if EMI is not considered.

In order to fully understand how weak signal detection performance of Izhikevich neuron is modulated by the chaotic current intensity ε and frequency of weak signal ω, the dependence of Q on ε and ω are calculated in a relatively wide range of the chaotic current intensity $\varepsilon \in$ [0-3.5] and the frequency of weak signal $\omega \in$ [0.001-1ms^{-1}]. It is seen that Figs. 5(a) and 5(b) show similar change rules on the

whole, i.e., a red area in which the weak signal can be best detected is observed. However, they also show differences in details. The range of maximum Q value in Fig. 5(a) is wider than that in Fig. 5(b), and the maximum value of Q is larger. A deeper analysis of the red region shows that the introduction of EMI makes Izhikevich neuron still have a certain response to weak signals when ε is small. These phenomena are completely consistent with the analysis results in Fig. 4, which shows that EMI has a certain impact on the detection ability of weak signal in Izhikevich neuron.

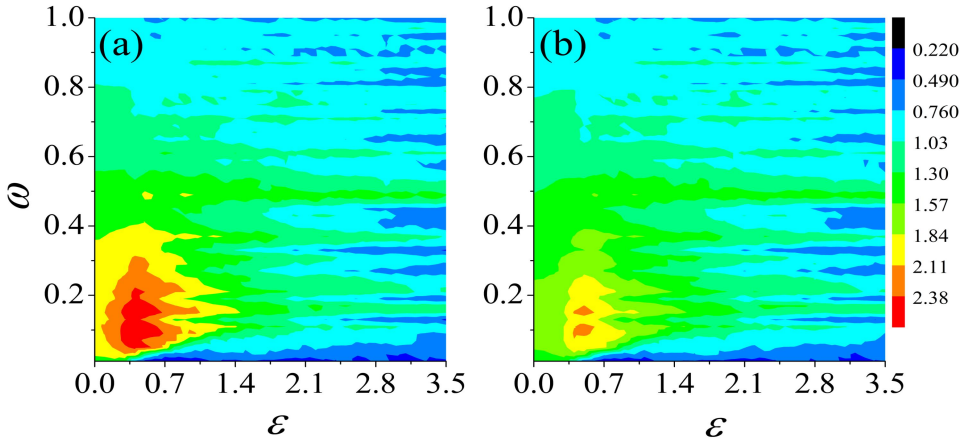

Fig. 5 Dependence of Q on chaotic current intensity ε and weak signal frequency ω at $A = 1.0$. (a) With the effects of EMI and $k_1 = 0.01$, $k_2 = 0.02$, $k_3 = 0.2$; (b) Without the effects of EMI.

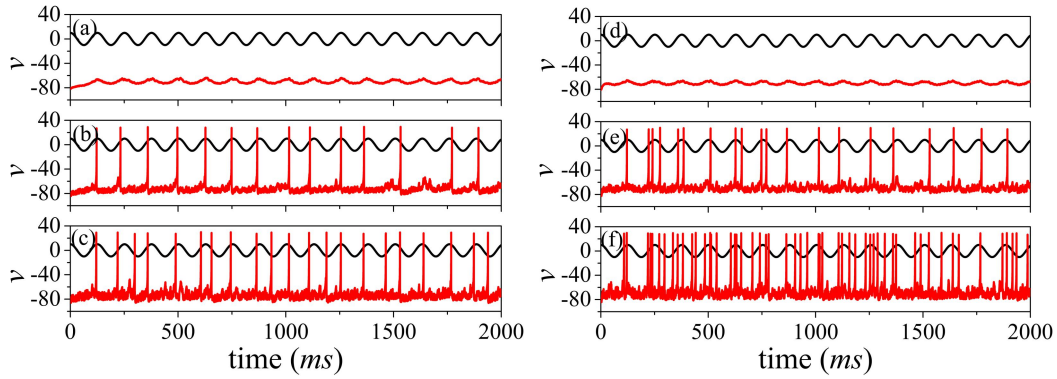

Fig. 6 The membrane potential of Izhikevich neuron and weak signal (the amplitude of weak signal is magnified 5 times for visibility) are plotted for three different chaotic current intensities at $A = 2.0$, $\omega = 0.05$: (a, d) $\varepsilon = 0.1$, (b, e) $\varepsilon = 0.6$, (c, f) $\varepsilon = 1.0$. The left panel is for RS neuron and the right panel is for FS neuron.

In order to provide a clearer perspective and explain the obtained results in more detail, the membrane potential of Izhikevich neuron and weak signal are presented as a function of time for three different chaotic current intensities. Among them, three chaotic current intensities of different sizes are defined as small value, intermediate value and large value, and their corresponding values are chosen as 0.1, 0.6 and 1.0,

respectively. For comparison, both FS and RS neuron cases are given in Fig. 6 and Fig. 7.

As illustrated in Fig. 6 and Fig. 7, the Izhikevich neuron is mostly in its quiescent state for small values of ε ($\varepsilon = 0.1$), and even one firing peak can not be seen.

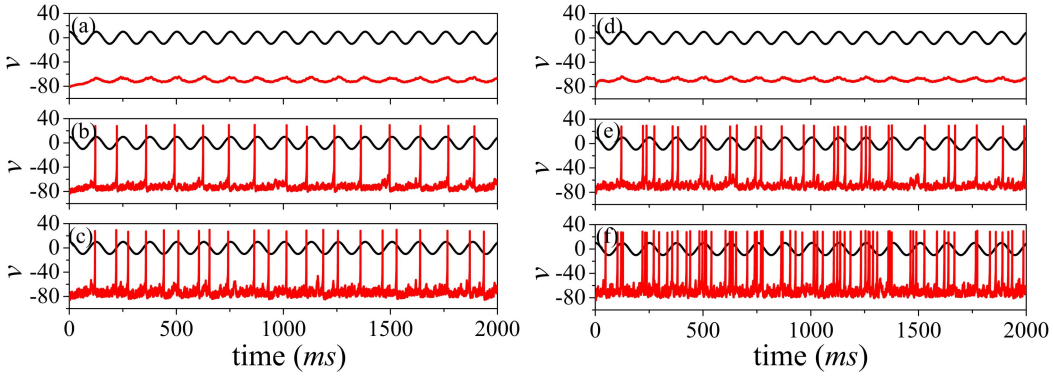

Fig. 7 The membrane potential of Izhikevich neuron and weak signal (the amplitude of weak signal is magnified 5 times for visibility) are plotted for three different chaotic current intensities under the effects of EMI at $A = 2.0$, $\omega = 0.05$, $k_1 = 0.01$, $k_2 = 0.02$, $k_3 = 0.2$: (a, d) $\varepsilon = 0.1$, (b, e) $\varepsilon = 0.6$, (c, f) $\varepsilon = 1.0$. The left panel is for RS neuron and the right panel is for FS neuron.

As we all know, neurons mainly rely on discharge spikes to transmit signals, so the Izhikevich neuron can not transmit any weak signals effectively for the given conditions here, that is, the input weak signal can not be detected at the output either. For the medium chaotic current intensity ($\varepsilon = 0.6$), one can see that the membrane potential at the output is strongly correlated with the input weak signal, and neuron fires a spike in each positive half cycle of weak signal resulting in a high encoding performance for the neuron. In this case, the weak signal received by neurons can be well detected.

Further increasing the chaotic current intensity to $\varepsilon = 1.0$, the time of neuron firing spike is no longer strongly correlated with the positive half cycle of weak signal. In this situation, the neuronal discharge activity does not match the period of weak signal, thus the disordered firing pattern is observed. Particularly, neuronal discharges can also be observed in the negative half cycle of weak signal, which indicates the lack of ability to detect weak signal. On the other hand, above results also show that large chaotic current intensity makes Izhikevich neuron in spiking state in the absence of weak signal. Another important conclusion is that FS neurons have faster firing rate than RS neurons. Therefore, FS neurons can fire more spikes under the optimal chaotic current intensity, indicating that they can carry and transmit more neural

information.

3.2 Chaotic resonance in Izhikevich neural network motifs

In early research, most of the researchers and scholars focuses on neuronal model and its numerical analysis. In the later research, complex networks in biological systems also aroused great interest of researchers. As far as the current situation is concerned, the complex networks studied mainly include feed-forward networks, small-world networks, scale-free networks and so on.

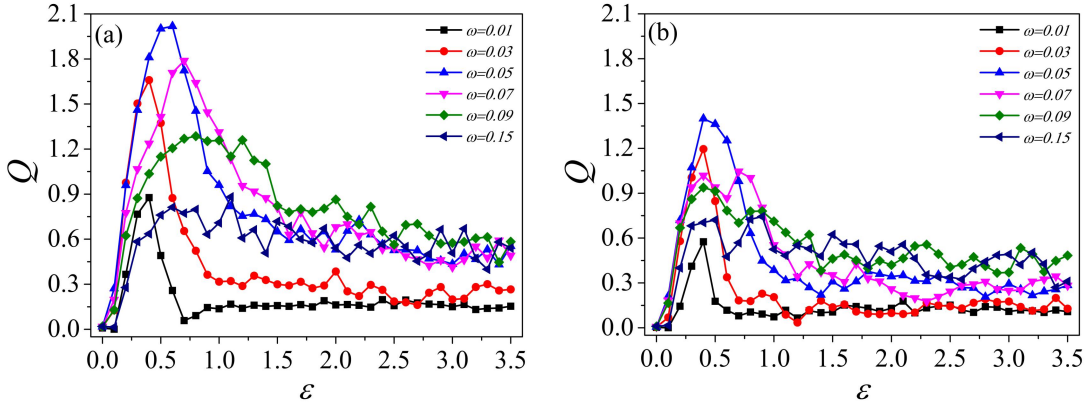

Fig. 8 Response of Izhikevich neural network motifs to weak signal (Q) are plotted as a function of chaotic current intensity ε for different weak signal frequency ω under the effects of EMI at A = 2.0, τ = 10, g = 0.9, k_1 = 0.01, k_2 = 0.02, k_3 = 0.2. (a) T1-FFL; (b) T2-FFL.

An unavoidable problem is that more and more studies show that some significant recurring nontrivial patterns of interconnections, termed as "network motifs", are the basic units of various complex neural networks. Since network motifs are considered to be basic building blocks of various neuronal networks, the function, neural information transmission or coding of network motifs have aroused widespread interest. In the following section, we will focus on the CR of Izhikevich neural network motifs under the effect of EMI.

As seen in Fig. 8, the response of Izhikevich neural network motifs to weak signal are plotted as a function of ε for different weak signal frequency ω under the effects of EMI. Considering the fact that meaningful results can be seen only when the input is excitatory neuron, the focus here is on T1-FFL and T2-FFL motif. It is obvious that the response curves of the two FFL network motifs to weak signals exhibit bell-shaped dependence on the chaotic current intensity, and the shape of this bell is more perfect, which indicates that the FFL coupled by three neurons plays a positive role in inducing CR.

Obtained results provide a profound enlightenment, that is, the triple-neuron FFL neuronal network motifs improve the signal detection and transmission ability in nervous system. So here comes the question: what about the information coding ability of the feedforward network composed of FFL? This question may be our further work to consider in the future, and the conclusion of this paper may provide inspiration for the answer to this question.

Numerical results in Fig.8 reveal a fact that there is an optimal chaotic current intensity (equaling approximately $\varepsilon = 0.6$ for T1-FFL motif and $\varepsilon = 0.4$ for T2-FFL motif) which can maximize Q if the frequency of weak signal is fixed. On the other hand, there is also an optimal weak signal frequency (equaling approximately $\omega = 0.05$) to maximize Q. Comparing these two types of FFL network motifs, it can be found that if the three neurons constituting the network motifs are all excitatory neurons (i.e. T1-FFL motif), the signal detection ability is better. The Q values of T2-FFL motif containing inhibitory neurons are smaller than T1-FFL network motif, indicating that inhibitory neurons in network weaken the ability of signal propagation in neural network motifs and inhibit the induction of CR.

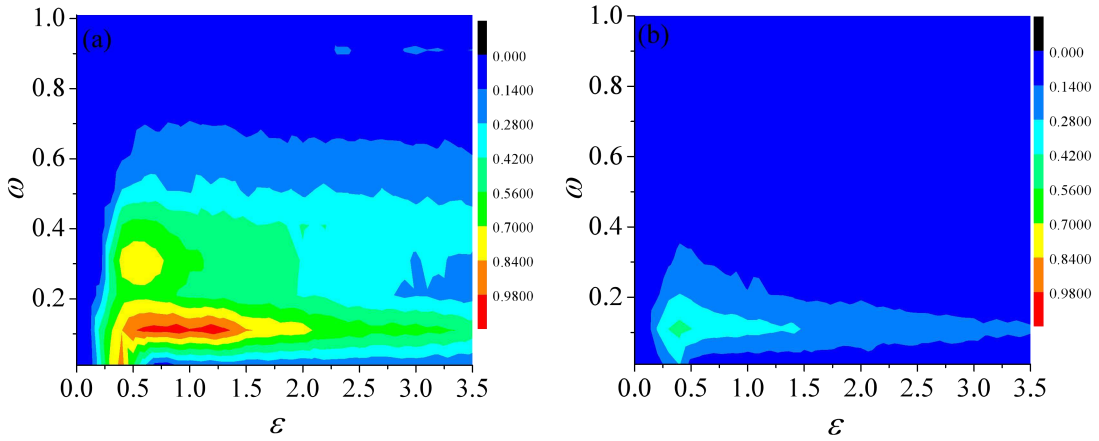

Fig. 9 Contour plot of the Fourier coefficient Q in parametric space (ε, ω) for Izhikevich neural network motifs under the effects of EMI at $A = 2.0$, $\tau = 10$, $g = 0.5$, $k_1 = 0.01$, $k_2 = 0.02$, $k_3 = 0.2$. (a) T1-FFL; (b) T2-FFL.

To fully understand the impact of weak signal frequency and chaotic current intensity for FFL network motifs, the contour plot of the Fourier coefficient Q in parametric space (ε-ω) for Izhikevich neural network motifs under the effects of EMI are presented in Fig. 9. The conclusion in Fig. 9 verifies that the detection performance of T1-FFL motif for weak signals is stronger than T2-FFL motif, and the range of parameters that maximize Q can also be found out intuitively.

For T1-FFL motif, the dependence of Q on chaotic current intensity and weak

signal frequency exhibits an obvious maximum, and a smaller extreme value (yellow area) appears near the maximum, which is defined as sub-harmonic resonance. For T2-FFL motif, most of the parameter areas are not able to guarantee the effective detection and transmission of weak signals. It is unearthed that the connection between inhibitory neurons and inhibitory synapses play an important role in the neural signals transmission. In addition, Fig. 9(b) also reveals a interesting phenomenon that no sub-harmonic resonance is observed in the contour plot of the Fourier coefficient Q in parametric space (ε,ω) for T2-FFL motifs.

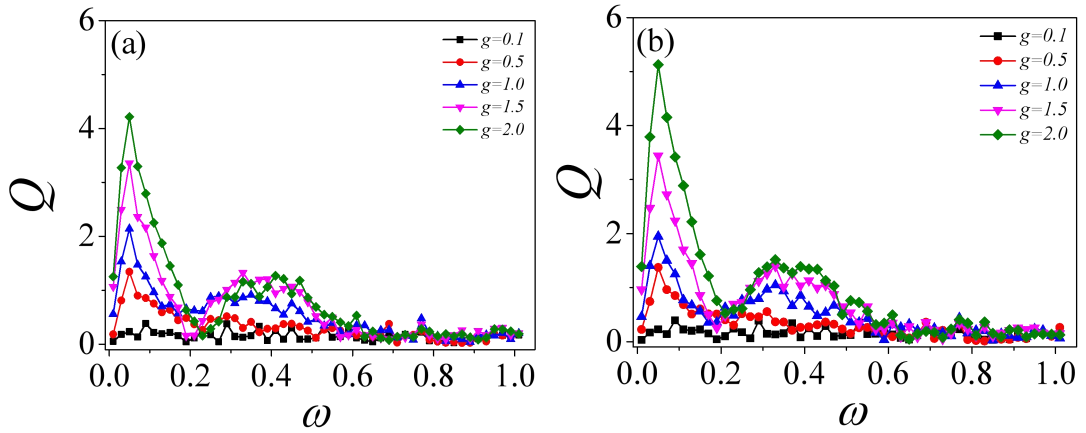

Fig. 10 Response of Izhikevich neural network motifs to weak signal (Q) is plotted as a function of frequencies ω of weak signal for different coupling strength g under the effects of EMI at A = 2.0, τ = 10, g = 0.1, k_1 = 0.01, k_2 = 0.02, k_3 = 0.2. (a) T1-FFL; (b) T2-FFL.

To further investigate the effects of weak signal frequency and coupling strength on the detect performance of Izhikevich neural network motifs, the response of zhikevich neural network motifs to weak signal is plotted as a function of weak signal frequencies ω for different coupling strength g under the effects of EMI, as presented in Fig. 10. Obviously, the curve of Q with respect to ω exhibits two maxima, of which the maximum on the left has the best signal detection ability, and the maximum on the right is called sub-harmonic resonance. But on the whole, there are two maxima in the Q curve, which can also be called chaotic double resonance. According to the definition of vibrational bi-resonance, this phenomenon can also be called chaotic bi-resonance. Another meaningful phenomenon is that the larger the coupling strength, the larger the corresponding Q value. This is consistent with the response of neural system to external stimulus. The larger the coupling strength represents the larger the signal input, and the corresponding response is also larger.

The phenomena of resonance, such as stochastic resonance, vibrational

resonance and chaotic resonance, in dynamical systems with time delay feedback have been widely studied in various fields. Especially in neuronal system, it was believed that time delay can induce multi-resonance and enhance neural synchronization. It was recently reported that different information transmission delays could induce stochastic resonance appear intermittently.

Generally speaking, due to the transmission of matter, energy and information, the time delay arises in dynamical system. In view of this, then the effect of time delay in synaptic variables on response of the system to weak signals is discussed. In order to investigate the effect of time delay feedback on dynamics of the system, the response of Izhikevich neural network motifs to weak signal are plotted as a function of time delay τ for different coupling strength g under the effects of EMI, as shown in Fig. 11.

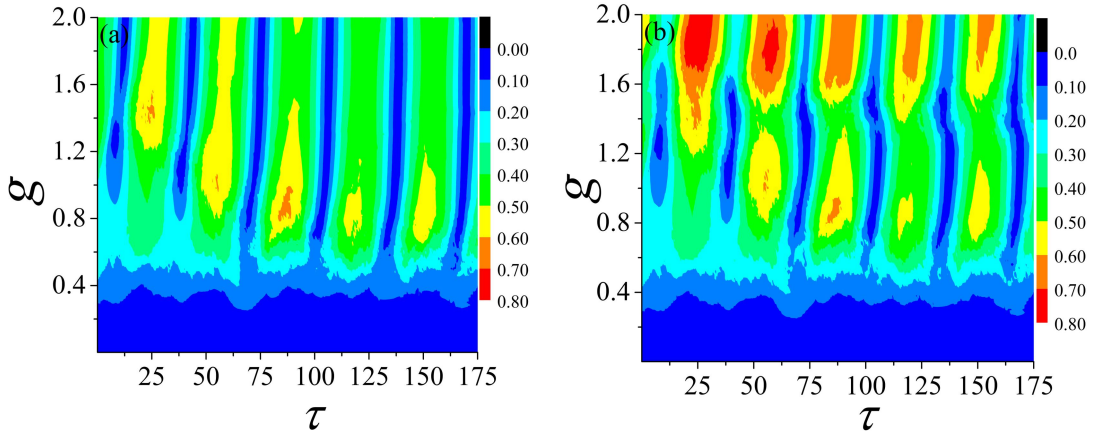

Fig. 11 Contour plot of the Fourier coefficient Q in parametric space (g, τ) for Izhikevich neural network motifs under the effects of EMI at $A = 2.0$, $\omega = 0.2$, $\varepsilon = 0.2$, $g = 0.5$, $k_1 = 0.01$, $k_2 = 0.02$, $k_3 = 0.2$. (a) T1-FFL; (b) T2-FFL.

It can be observed from Fig. 11 that there exist some bright strip-like regions of high values of Q, where CR can be realized. Where resonance occurs, neurons fire and information can be transmitted. From an overall perspective, one can confirm that a periodic resonance behavior with the period approximately equal to $28ms$ for the system is found, which can be defined as quasi periodic chaotic resonance (QPCR). Indeed, with the increasing of information transmission time delay, T1-FFL motif exhibits intermittent appearance of CR.

The response of T2-FFL motifs to weak signal is generally the same with T1-FFL motifs, but it also shows different aspects. On the whole, the contour plot of the Fourier coefficient Q versus parameters (g, t) still shows the characteristics of QPCR, along with roughly the same period. For small coupling strength, the response

of both T1-FFL and T2-FFL motifs to weak signal are low regardless of the delay time. However, when the coupling strength g is relatively large (for $g > 1.5$), the Q value of some parameter regions of T2-FFL is larger than T1-TTL, as shown in the red region in Fig. 11(b). The above conclusions verify again that time delay can not only promote and improve the synchronization of neurons, but also induce multiple resonance leading to many interesting phenomena. Further, these analyses tell us that the time delay mainly originate from the limited speed of action potential propagation on neuronal axons and the time delay of dendritic and synaptic processes are inevitable in intermediate neuronal communication and inherent in the nervous system, so it is worth discussing.

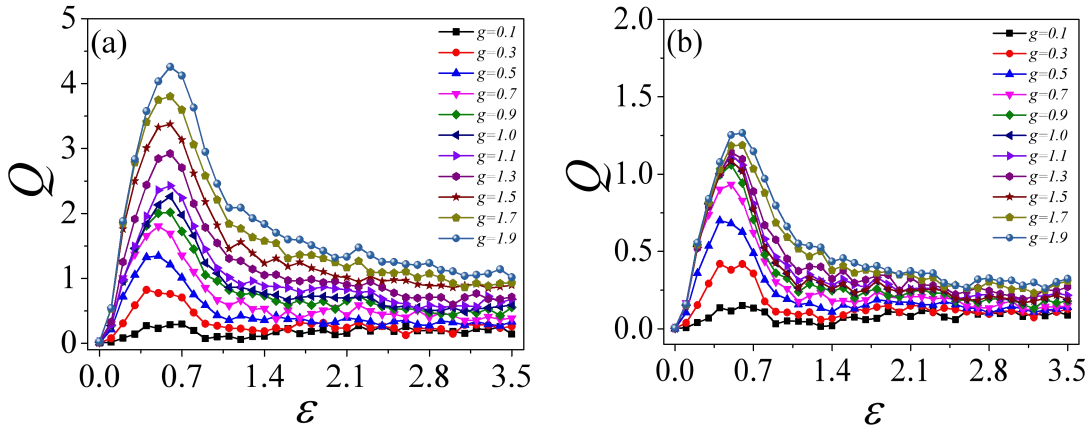

Fig. 12 Response of Izhikevich neural network motifs to weak signal (Q) are plotted as a function of ε for different coupling strength g under the effects of EMI at $A = 2.0$, $\tau = 10$, $\omega = 0.05$, $k_1 = 0.01$, $k_2 = 0.02$, $k_3 = 0.2$. (a) T1-FFL; (b) T2-FFL.

The coupling strength determines the strength of the connection between neurons, so it is also of practical significance to investigate the influence of coupling strength on system response. As depicted in Fig. 12, the dependence of Fourier coefficient Q on chaotic current intensity ε are presented. With the increase of chaotic current intensity ε, the Q-ε curve shows a perfect bell-shape relationship, which indicates the occurrence of CR. The maximum in Q curve represents the best chaotic current intensity that optimize the weak signal detection performance of neural network motifs. Moreover, it can be seen that the larger the coupling strength g, the higher the peak height of the Q curve. However, large coupling strength may lead to the too fast discharge of neurons that make up the neural network motifs, hence too large coupling strength is not discussed here.

On the other hand, the Q value of T2-FFL motif is much smaller than that of T1-FFL motif, indicating that the addition of inhibitory neuron to neural network

motif has a great impact on signal detection performance of the neural network motifs. When the signal is transmitted directly from neuron 1 to neuron 3, the information transmission efficiency will not decrease. However, if weak signals are transmitted from neuron 1 to neuron 2 and then to neuron 3, the propagation efficiency decreases because neuron 2 is an inhibitory neuron. Above results can provide some theoretical support for the construction of neural network, so that one can clearly know how to build neural network better.

3.3 Effects of electromagnetic induction on chaotic resonance in Izhikevich neural network motifs

As a new physical quantity introduced into neural model, EMI has attracted the attention of a large number of researchers. Considering the widespread existence of EMI, it is of practical significance to discuss the influence of EMI on CR of neural network motifs. Results shown in Fig. 13 clarify the findings that the Q curves of T1-FFL and T2-FFL neural network motifs exhibit resonance-like behaviors dependence on k_1, and they have the same change trend with the increasing of k_1, that is, a smaller maximum appears first, and then a larger maximum appears. The first maximum of Q for T1-FFL motif occurs when $k_1 = 0.06$ ($k_1 = 0.10$ for T2-FFL motif), while the second maximum occurs when $k_1 = 0.24$ ($k_1 = 0.26$ for T2-FFL motif).

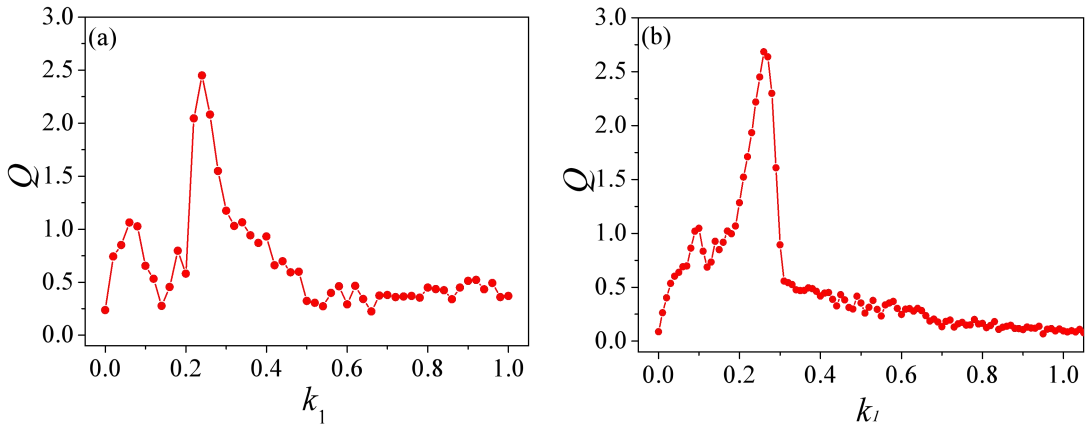

Fig. 13 Response of Izhikevich neural network motifs to weak signal (Q) are plotted as a function of k_1 under the effects of EMI at $A = 2.0$, $\tau = 10$, $\omega = 0.2$, $g = 0.5$, $\varepsilon = 0.3$, $k_2 = 0.02$, $k_3 = 0.2$. (a) T1-FFL; (b) T2-FFL.

For T1-FFL motif, the Q value drops to a lower level when the value of k_1 is larger than 0.54, which means that too large k_1 value is not conducive to the detection of weak signals. However, for T2-FFL motif, the Q value quickly decreases to a lower

level when the value of k_1 is larger than 0.31, and continues to decrease approximately equal to 0 with the increase of k_1. If the value of Q is equal to 0, it means that the detection performance of neural network motifs for weak signals is significantly diminished, or even tends to disappear. Above results show that there is an optimal EMI, which can make the signal detection ability of neural network motifs best. Furthermore, too strong EMI may destroy the information coding function of neural network motifs, resulting in the lack of signal detection ability.

The term $k_2 v$ in Eq. (5) represents the influence of membrane on magnetic flow, and $k_3 \varphi$ describes the leakage of magnet flux. Then the response of Izhikevich neural network motifs to weak signal are plotted as a function of k_2 and k_3 under the effects of EMI, as displayed in Figs. 14-15.

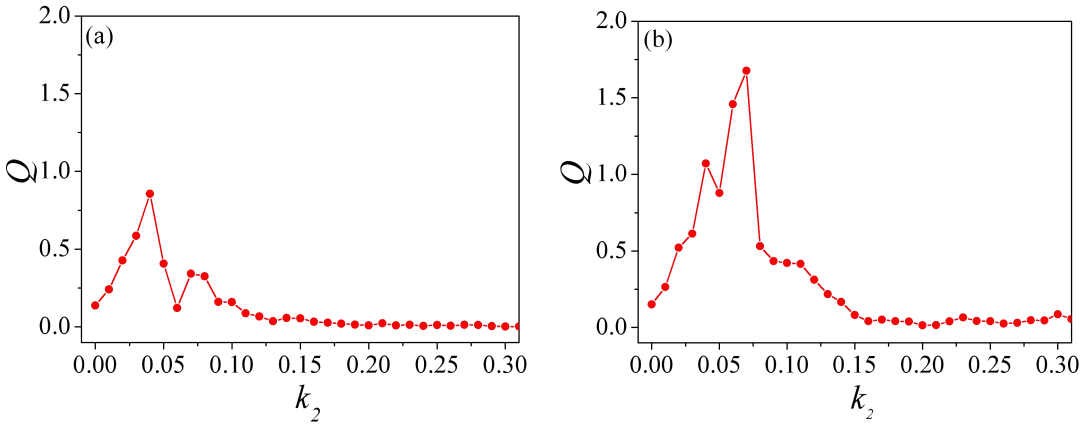

Fig. 14 Response of Izhikevich neural network motifs to weak signal (Q) are plotted as a function of k_2 under the effects of EMI at $A = 2.0$, $\tau = 10$, $\omega = 0.2$, $g = 0.5$, $\varepsilon = 0.3$, $k_1 = 0.01$, $k_3 = 0.2$. (a) T1-FFL; (b) T2-FFL.

It is clearly seen that the weak signal detection performance of both T1-FFL and T2-FFL neural network motifs display a resonance-like dependence on k_2 and k_3. For the two different FFL neural network motifs discussed here, the Q value of T2-FFL motif is larger than that of T1-FFL motif under the same parameter conditions. Thus, one can conclude that changing the parameters of EMI or external current input (including chaotic current and weak signal current) has different effects on detection performance of the two FFL neural network motifs. Through the comparison between sections 3.2 and 3.3, it can be found that the detection performance of T1-FFL motif for weak signal is better than T2-FFL motif when the parameters of external current are changed. However, the detection performance of T2-FFL motif for weak signal is in turn stronger than T1-FFL motif when the parameters of EMI are changed.

As can be seen from Fig. 14, the Q curve shows a resonance-like dependence on k_2, with the maximum value of Q for T1-FFL motif appears at k_2 = 0.04 and the maximum value of Q for T2-FFL motif appears at k_2 = 0.07. However, it is coincidentally found that the k_3 value which maximize Q are obtained at k_3 = 0.03 for both T1-FFL and T2-FFL neural network motifs, as shown in Fig. 15.

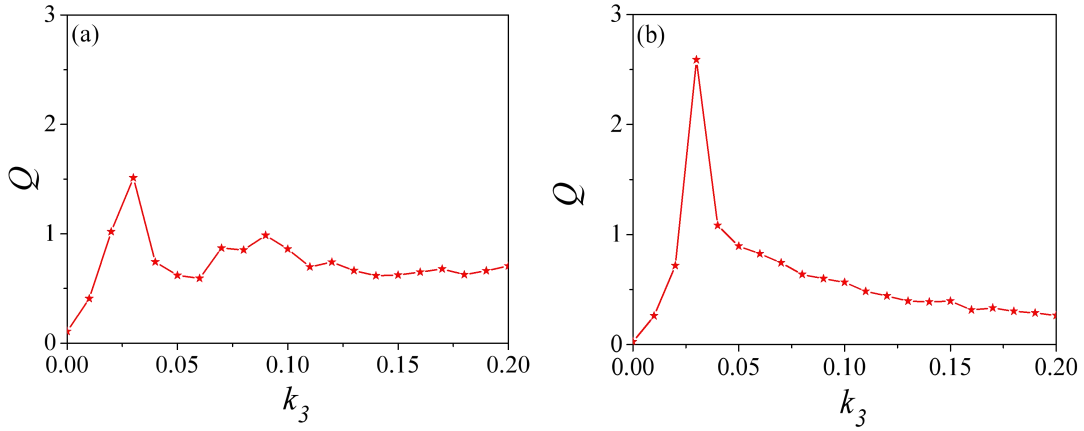

Fig. 15 Response of Izhikevich neural network motifs to weak signal (Q) are plotted as a function of k_3 under the effects of EMI at A = 2.0, τ = 10, ω = 0.2, g = 0.5, ε = 0.3, k_1 = 0.01, k_2 = 0.01. (a) T1-FFL; (b) T2-FFL.

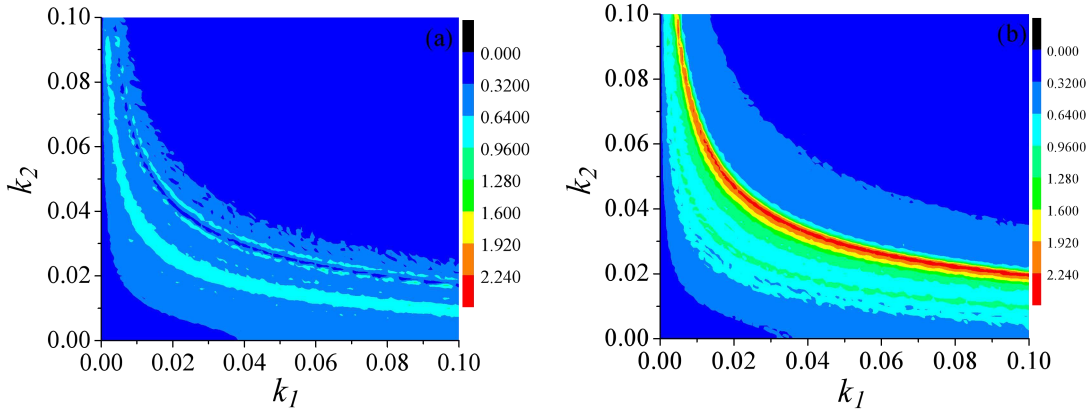

Fig. 16 Contour plot of Q in k_1-k_2 parameters plane under the effects of EMI at A = 2.0, τ = 10, ω = 0.2, g = 0.5, ε = 0.3, k_3 = 0.2. (a) T1-FFL; (b) T2-FFL.

In order to fully understand the influence of EMI on CR, the contour plot of Q in k_1-k_2 parameters plane under the effects of EMI for both T1-FFL and T2-FFL neural network motifs are depicted in Fig. 16. Since the k_2 value corresponding to the maximum value of Q is small, and large k_2 value has an adverse impact on signal detection performance of neural network motifs. Therefore, only the influence of small k_1 and k_2 values (k_1 and $k_2 \in [0,0.1]$) on Q is considered. It is found that a series of striped ribbons are observed, and the Q value of T2-FFL motif is obviously larger than that of T1-FFL motif.

4. Conclusions

An improved Izhikevich neuronal model in the presence of EMI is proposed, and the triple-neuron FFL neural network motifs are constructed in this paper. The CR phenomenon of Izhikevich neural model under the effects of EMI is discussed by calculating the response amplitude of chaotic signal to weak signal input the system, and the detection performance of FFL neural network motifs composed of excitatory and inhibitory Izhikevich neurons for weak signals is studied. Meanwhile, how EMI affects the CR of single Izhikevich neuron and its neural network motifs is also explored in detail.

Obtain results show that there exists an optimal chaotic current intensity, which can make the single Izhikevich neuron have the best detection performance for weak signals. Further results uncover the fact that the introduction of EMI enhances the ability of single Izhikevich neuron to detect weak signals. It can be seen from the time series of membrane potential of RS and FS neurons that the most coherent firings with the weak signal occur at the intermediate level of chaotic current intensity, this is consistent with the phenomenon that the Fourier coefficient exhibits bell-shaped dependence on the chaotic current intensity. When the CR for T1-FFL and T2-FFL neural network motifs are checked under the effects of EMI, it is found that the detection performance of T2-FFL motifs to weak signals is worse than T1-FFL motifs due to the existence of inhibitory neurons. Furthermore, the effect of time delay in synaptic variables on response of the neural network motifs to weak signals is discussed, and the quasi periodic CR is observed with the increasing of information transmission time delay. In addition, the influence of EMI on CR has also been studied in detail, and one can conclude that the introduce of EMI enhances the weak signal detection performance of T2-FFL neural network motifs regardless of the presence of inhibitory neurons.

Results in this paper have revealed that CR effect is a robust phenomenon which can be observed both in single Izhikevich neuron and network motifs, and these conclusions can help people understand how to improve the ability of weak signal detection and propagation in chaotic neuronal system.

Acknowledgement

This project is supported by National Natural Science Foundation of China under Grants Nos 12175080 and 11775091.

Compliance with ethical standards

Data Availability Statement

All data generated or analysed during this study are included in this published article.

Conflict of interest

The authors declare that they have no potential conflict of interest.

References

[1] McNamara, B., Wiesenfeld, K.: Theory of stochastic resonance. Phys. Rev. A 39(9): 4854-4869 (1989).
[2] Hänggi, P., Jung, P., Zerbe, C., *et al*.: Can colored noise improve stochastic resonance. J. Stat. Phys. 70(1-2): 25-47 (1993).
[3] Jia, Y., Yu, S.N., Li, J.R.: Stochastic resonance in a bistable system subject to multiplicative and additive noise. Phys. Rev. E 62(2): 1869-1878 (2000).
[4] Stocks, N.G., Stein, N.D., Mcclintock, P.: Stochastic resonance in monostable systems. J. Phys. A Gen. Phys. 26(7): L385-L390 (1993).
[5] Benzi, R., Parisi, G., Sutera, A., *et al*.: Stochastic resonance in climatic change. Tellus 34(1): 10-15 (1982).
[6] Dykman, M.I., Mannella, R., Mcclintock, P., et al.: Phase shifts in stochastic resonance. Phys. Rev. Lett. 68(20): 2985-2988 (1992).
[7] Yu, D., Lu, L.L., Wang, G.W., *et al*.: Synchronization mode transition induced by bounded noise in multiple time-delays coupled FitzHugh-Nagumo model. Chaos Solitons Fractals. 147(4): 111000 (2021).
[8] Yao, C., Ma, J., He, Z., *et al*.: Transmission and detection of biharmonic envelope signal in a feed-forward multilayer neural network. Physica A. 523: 797-806 (2019).
[9] Yilmaz, E., Ozer, M.: Delayed feedback and detection of weak periodic signals in a stochastic Hodgkin-Huxley neuron. Physica A. 421(1): 455-462 (2015).
[10] Yao, Y., Su, C., Xiong, J.: Enhancement of weak signal detection in the Hodgkin–Huxley neuron subjected to electromagnetic fluctuation. Physica A. 531: 121734 (2019).
[11] Hänggi, P.: Stochastic resonance in biology how noise can enhance detection of weak signals and help improve biological information processing. Chem. Phys. Chem. 3(3): 285-290 (2015).
[12] McInnes, C.R., Gorman, D.G., Cartmell, M.P.: Enhanced vibrational energy harvesting using nonlinear stochastic resonance. J. Sound Vib. 318(4-5): 655-662 (2008).
[13] Liu, Y., Dai, Z., Lu, S, *et al*.: Enhanced bearing fault detection using step-varying vibrational resonance based on Duffing oscillator nonlinear system. Shock and Vibration. 2017(PT.5): 1-14 (2017).
[14] Landa, P.S., Mcclintock, P.: Vibrational resonance. J. Phys. A Gen. Phys. 33(45): L433-L438 (2000).
[15] Lu, L.L., Jia, Y., Ge, M.Y., *et al*.: Inverse stochastic resonance in Hodgkin-Huxley neural system driven by Gaussian and non-Gaussian colored noises. Nonlinear Dyn. 100(1): 877-889

(2020).
[16] Yang, J.H., Liu, X.B.: Delay induces quasi-periodic vibrational resonance. J. Phys. A Math. Theor. 43(12): 122001 (2010).
[17] Xue, M., Wang, J., Deng, B., *et al*.: Vibrational resonance in feedforward neuronal network with unreliable synapses. Eur. Phys. J. B. 86(4): 1-9 (2013).
[18] Wang, G.W., Yu, D., Ding, Q.M., *et al*.: Effects of electric field on multiple vibrational resonances in Hindmarsh-Rose neuronal systems. Chaos Solitons Fractals. 150(9): 111210 (2021).
[19] Wang, C.J.: Vibrational resonance in an overdamped system with a sextic double-well potential. Chin. Phys. Lett. 28(9): 090504 (2011).
[20] Wang, C., Yang, K., Qu, S.: Vibrational resonance in a discrete neuronal model with time delay. Int. J. Mod. Phys. B. 28(16): 1450103 (2014).
[21] Deng, B., Deng, Y., Yu, H., *et al*.: Dependence of inter-neuronal effective connectivity on synchrony dynamics in neuronal network motifs. Chaos Solitons Fractals. 82(1): 48-59 (2016).
[22] Lou, X.: Stochastic resonance in neuronal network motifs with Ornstein-Uhlenbeck colored noise. Math. Probl. Eng. 2014: 1-7 (2014).
[23] Dong, C., Chen, X.: Study of robustness of synchronized bursting behaviors for spike neural network motifs. J. Comput. (8): 71-84 (2012).
[24] Uzuntarla, M., Yilmaz, E., Wagemakers, A., *et al*.: Vibrational resonance in a heterogeneous scale free network of neurons. Commun. Nonlinear Sci. Numer. Simul. 22(1-3): 367-374 (2015).
[25] Ullner, E., Zaikin, A., GarcÕa-Ojalvo, J., *et al*.: Vibrational resonance and vibrational propagation in excitable systems. Phys. Lett. A. 312(5-6): 348-354 (2003).
[26] Sun, J., Deng, B., Liu, C., *et al*.: Vibrational resonance in neuron populations with hybrid synapses. Appl. Math. Model. 37(9): 6311-6324 (2013).
[27] Chizhevsky, V.N.: Experimental evidence of vibrational resonance in a multistable system. Phys. Rev. E. 89(6): 062914 (2014).
[28] Ibrahim, R.I., Naimee, K., Sammer, K.Y.: Experimental evidence of chaotic resonance in semiconductor laser. Baghdad Science Journal. 18(1): 2411-7986 (2021).
[29] Chew, L.Y., Ting, C., Lai, C.H.: Chaotic resonance: two-state model with chaos-induced escape over potential barrier. Phys. Rev. E. 72(3): 036222 (2005).
[30] Baysal, V., Saraç, Z., Yilmaz, E.: Chaotic resonance in Hodgkin-Huxley neuron. Nonlinear Dyn. 97(1): 1275-1285 (2019).
[31] Baysal, V., Erkan, E., Yilmaz, E.: Impacts of autapse on chaotic resonance in single neurons and small-world neuronal networks. Philos. Trans. R. Soc. Lond. A. 379: 20200237 (2021).
[32] Tokuda, I.T., Han, C.E., Aihara, K., *et al*.: The role of chaotic resonance in cerebellar learning. Neural Netw. 23(7): 836-842 (2010).
[33] Nobukawa, S., Nishimura, H.: Chaotic resonance in coupled inferior olive neurons with the llinas approach neuron model. Neural Comput. 28(11): 2505-2532 (2016).
[34] Ishimura, K., Asai, T., Motomura, M.: Chaotic resonance in forced Chua's oscillators. J. Signal Process. 17(6): 231-238 (2013).
[35] Djomo Mbong, T.L.M., Siewe, M., Tchawoua, C.: The effect of nonlinear damping on vibrational resonance and chaotic behavior of a beam fixed at its two ends and prestressed. Commun. Nonlinear Sci. Numer. Simul. 22(1-3): 228-243 (2015).
[36] Wang, M.S., Hou, Z.H., Xin, H.W.: Synchronization and coherence resonance in chaotic neural networks. Chin. Phys. 15(11): 2553 (2006).
[37] Anishchenko, V.S., Neiman, A.B., Safanova, M.A.: Stochastic resonance in chaotic systems. J. Stat. Phys. 70(1-2): 183-196 (1993).
[38] Nobukawa, S., Nishimura, H., Yamanishi, T., *et al*.: Chaotic states induced by resetting process in Izhikevich neuron model. J. Artif. Intell. Soft Comput. Res. 5(2): 109-119 (2015).
[39] Jiao, Z.Q., Zou, L., Cao, Y., *et al*.: Effective connectivity analysis of fMRI data based on network motifs. J. Supercomput. 67(3): 806-819 (2014).
[40] Milo, R., Shen-Orr, S., Itzkovitz, S., *et al*.: Network motifs: simple building blocks of complex networks. Science. 298(5594): 824-827 (2002).
[41] Alon, U.: Network motifs: theory and experimental approaches. Nat. Rev. Genet. 8(6): 450-461 (2007).
[42] Shin, M.M., Sano, T., Nonmembers, T.U., *et al*.: Resonance in a chaotic neuron model driven by a weak sinusoid. IEICE Trans. on Fundamentals. E82-A(4): 671-679 (1999).
[43] Yao, Y.G., Ma, J., Gui, R., *et al*.: Enhanced logical chaotic resonance. Chaos. 31(2): 023103

(2021).
[44] Ambika, G., Menon, K., Harikrishnan, K.P.: Aspects of stochastic resonance in Josephson junction, bimodal maps and coupled map lattice. Pramana. 64(4): 535-542 (2005).
[45] Castro, R., Sauer, T.: Chaotic stochastic resonance: noise-enhanced reconstruction of attractors. Phys. Rev. Lett. 79(6): 1030-1033 (1997).
[46] Wooyoung, K., Min, L., Wang, J., *et al*.: Biological network motif detection and evaluation. BMC Syst. Biol. 5(S5): S5 (2011).
[47] Dong, C., Chen, X.: Study of Robustness of Synchronized Bursting Behaviors for Spike Neural Network Motifs. J. Comput. 7(8): 71-84 (2012).
[48] Izhikevich, E.M., Gally, J.A., Edelman, G.M.: Spike-timing dynamics of neuronal groups. Cereb Cortex. 8: 933-944 (2004).
[49] Song, X.L., Wang, H.T., Chen, Y.: Coherence resonance in an autaptic Hodgkin-Huxley neuron with time delay. Nonlinear Dyn. 94(1): 141-150 (2018).
[50] Teka, W.W., Upadhyay, R.K., Mondal, A.: Spiking and bursting patterns of fractional-order Izhikevich model. Commun. Nonlinear Sci. Numer. Simul. 56: 161-176(2018).
[51] Nobukawa, S., Nishimura, H., Yamanishi, T., *et al*.: Analysis of chaotic resonance in Izhikevich neuron model. PLoS One. 10(9): e0138919 (2015).
[52] Kafraj, M.S., Parastesh, F., Jafari, S.: Firing patterns of an improved Izhikevich neuron model under the effect of electromagnetic induction and noise. Chaos Solitons Fractals. 137(8): 109782 (2020).
[53] Nobukawa, S., Nishimura, H., Yamanishi, T.: Chaotic resonance in typical routes to chaos in the Izhikevich neuron model. Sci. Rep. 7(1): 1331 (2017).
[54] Ge, M.Y., Jia, Y., Lu, L.L., *et al*.: Propagation characteristics of weak signal in feedforward Izhikevich neural networks. Nonlinear Dyn. 99(4): 2355-2367 (2019).
[55] Yang, Y.M., Ma, J., Xu, Y., *et al*.: Energy dependence on discharge mode of Izhikevich neuron driven by external stimulus under electromagnetic induction. Cogn. Neurodyn. 15(2): 265-277 (2021).
[56] Hindmarsh, J., Rose, R.: A model of the nerve impulse using two first-order differential equations. Nature. 296(5853): 162-164 (1982).
[57] Kim, S.Y., Kim, Y., Hong, D.G., *et al*.: Stochastic bursting synchronization in a population of subthreshold Izhikevich neurons. J. Korean Phys. Soc. 60(9): 1441-1447 (2012).
[58] Ge, M.Y., Lu, L.L., Xu, Y., *et al*.: Vibrational mono-/bi-resonance and wave propagation in FitzHugh-Nagumo neural systems under electromagnetic induction. Chaos Solitons Fractals. 133(4): 109645 (2020).
[59] Hou, Z.L., Ma, J., Zhan, X., *et al*.: Estimate the electrical activity in a neuron under depolarization field. Chaos Solitons Fractals. 142(4): 110522 (2020).
[60] Elkaranshawy, H.A., Aboukelila, N.M., Elabsy, H.M.: Suppressing the spiking of a synchronized array of Izhikevich neurons. Nonlinear Dyn. 104(1): 2653-2670 (2021).
[61] Xu, Y., Ma, J., Zhan, X., *et al*.: Temperature effect on memristive ion channels. Cogn. Neurodyn. 13(11): 601-611 (2019).
[62] Kim, S.Y., Woochang, L.: Coupling-induced population synchronization in an excitatory population of subthreshold Izhikevich neurons. Cogn. Neurodyn. 7(6): 495-503 (2013).
[63] Tamura, A., Ueta, T., Tsuji, S.: Bifurcation analysis of Izhikevich model. Dynamics of Continuous, Discrete and Impulsive Systems Series A: Mathematical Analysis. 16(6): 849-862 (2009).
[64] Izhikevich, E.M.: Simple model of spiking neurons. IEEE Trans. Neural Netw. 14(6): 1569-72 (2003).
[65] Benayoun, M., Cowan, J.D., Drongelen, W.V., *et al*.: Avalanches in a stochastic model of spiking neurons. PLoS Comput. Biol. 6(7): e1000846 (2010).
[66] Leveille, J., Versace, M., Grossberg, S.: Running as fast as it can: How spiking dynamics form object groupings in the laminar circuits of visual cortex. J. Comput. Neurosci. 28(2): 323-346 (2010).
[67] Zhou, X.Y., Xu, Y., Wang, G.W., *et al*.: Ionic channel blockage in stochastic Hodgkin-Huxley neuronal model driven by multiple oscillatory signals. Cogn. Neurodyn. 14(4): 569-578 (2020).
[68] Wu, F.Q., Wang, C.N., Jin, W.Y., *et al*.: Dynamical responses in a new neuron model subjected to electromagnetic induction and phase noise. Physica A. 469: 81-88 (2017).
[69] Ge, M.Y., Wang, G.W., Jia, Y., *et al*.: Influence of the Gaussian colored noise and

784 electromagnetic radiation on the propagation of subthreshold signals in feedforward neural
785 networks. Sci. China Technol. Sci. 64(4): 847-857 (2021).
786 [70] Thackston, K.A., Deheyn, D.D., Sievenpiper, D.F.: Limitations on electromagnetic
787 communication by vibrational resonances in biological systems. Phys. Rev. E. 101(6-1): 062401
788 2020.
789 [71] Zhang, X.H., Liu, S.Q.: Stochastic resonance and synchronization behaviors of excitatory
790 inhibitory small-world network subjected to electromagnetic induction. Chin. Phys. B. V27(04):
791 202-211 (2018).
792 [72] Rajagopal, K., Moroz, I., Karthikeyan, A., *et al*.: Wave propagation in a network of extended
793 Morris-Lecar neurons with electromagnetic induction and its local kinetics. Nonlinear Dyn. 100(4):
794 3625-3644 (2020).
795 [73] Baysal, V., Yilmaz, E.: Effects of electromagnetic induction on vibrational resonance in
796 single neurons and neuronal networks. Physica A. 537: 122733 (2020).
797 [74] Liu, C., Wang, J., Yu, H., *et al*.: The effects of time delay on the stochastic resonance in
798 feed-forward-loop neuronal network motifs. Commun. Nonlinear Sci. Numer. Simul. 19(4):
799 1088-1096 (2014).
800 [75] Li, C.: Functions of neuronal network motifs. Phys. Rev. E. 78(3): 037101 (2008).
801 [76] Kopelowitz, E., Abeles, M., Cohen, D., *et al*.: Sensitivity of global network dynamics to local
802 parameters versus motif structure in a cortexlike neuronal model. Phys. Rev. E. 85(5): 051902
803 (2012).
804 [77] Kashtan, N., Itzkovitz, S., Milo, R., *et al*.: Topological generalizations of network motifs.
805 Phys. Rev. E. 70(3 Pt 1): 031909 (2003).
806 [78] Hobert, O.: Regulatory logic of neuronal diversity: Neuronal selector genes and selector
807 motifs. Dev. Biol. 105(51): 20067-20071 (2008).
808 [79] Ahnert, S.E., Fink, T.M.: Form and function in gene regulatory networks: the structure of
809 network motifs determines fundamental properties of their dynamical state space. J. R. Soc.
810 Interface. 13(120): 20160179 (2016).
811 [80] Grossberg, S.: How does the cerebral cortex work? Learning, attention, and grouping by the
812 laminar circuits of visual cortex. Spat. Vis. 12(2): 163 (1999).
813 [81] Izhikevich, E.M.: Which model to use for cortical spiking neurons? IEEE Trans. Neural Netw.
814 15(5): 1063-1070 (2004).
815 [82] Wang, G.W., Ge, M.Y. Lu, L.L., *et al*.: Study on propagation efficiency and fidelity of
816 subthreshold signal in feed-forward hybrid neural network under electromagnetic radiation.
817 Nonlinear Dyn. 103(3): 2627-2643 (2021).
818 [83] Makarov, V.A., Calvo, C., Gallego, V., *et al*.: Synchronization of Heteroclinic Circuits
819 Through Learning in Chains of Neural Motifs. IFAC PapersOnLine. 49(14): 80-83 (2016).
820 [84] Ning, L., Chen, Z.: Vibrational resonance analysis in a gene transcriptional regulatory system
821 with two different forms of time-delays. Physica D. 401(1): 132164 (2020).
822 [85] Hu, D., Yang, J., Liu, X.: Delay-induced vibrational multiresonance in FitzHugh-Nagumo
823 system. Commun. Nonlinear Sci. Numer. Simul. 17(2): 1031-1035 (2012).
824 [86] Ning, L., Guo, W..: The influence of two kinds of time delays on the vibrational resonance of
825 a fractional Mathieu-Duffing oscillator. Pramana. 94(1): 40 (2020).
826 [87] Yang, J.H., Liu, X.B.: Controlling vibrational resonance in a multistable system by time delay.
827 Chaos. 20(3): 1501 (2010).
828 [88] Wang, G.W., Xu, Y., Ge, M.Y., *et al*.: Mode transition and energy dependence of
829 FitzHugh-Nagumo neural model driven by high-low frequency electromagnetic radiation. Int. J.
830 Electron. Commun. 120(6): 153209 (2020).
831 [89] Machado, J.N., Matias, F.S.: Phase bistability between anticipated and delayed
832 synchronization in neuronal populations. Phys. Rev. E. 102: 032412 (2020).
833 [90] Porta, L.D., Matias, F.S., Dos Santos, A.J., *et al*.: Exploring the Phase-Locking Mechanisms
834 Yielding Delayed and Anticipated Synchronization in Neuronal Circuits. Front Syst. Neurosci. 13:
835 41 (2019).